The British Journal of Radiology, 85 (2012), 745–752

Assessment of ablative margin by MRI with ferucarbotran in radiofrequency ablation for liver cancer: comparison with enhanced CT

[1]S TOKUNAGA, MD, [1]M KODA, PhD, MD, [1]T MATONO, PhD, MD, [1]T SUGIHARA, PhD, MD, [1]T NAGAHARA, PhD, MD, [1]M UEKI, PhD, MD, [1]Y MURAWAKI, PhD, MD, [2]S KAKITE, MD and [2]E YAMASHITA, PhD

[1]*Division of Medicine and Clinical Science, Department of Multidisciplinary Internal Medicine, Tottori University School of Medicine, Yonago, Japan, and* [2]*Division of Radiology, Department of Pathophysiological and Therapeutic Science, Tottori University School of Medicine, Yonago, Japan*

Objectives: Our aim was to determine whether ablated liver parenchyma surrounding a tumour can be assessed by MRI with ferucarbotran administered prior to radiofrequency ablation (RFA) compared with enhanced CT.
Methods: 55 hepatocellular carcinomas (HCCs) in 42 patients and 5 metastatic liver cancers in 3 patients were treated by RFA after ferucarbotran administration. We then performed T_2* weighted MRI after 1 week and enhanced CT after 1 month. T_2* weighted MRI demonstrated the ablated parenchyma as a low-intensity rim around the high intensity of the ablated tumour in these cases. The assessment was allocated to one of three grades: margin (+), high-intensity area with continuous low-intensity rim; margin zero, high-intensity area with discontinuous low-intensity rim; and margin (−), high-intensity area extending beyond the low-intensity rim.
Results: Margin (+), margin zero and margin (−) were found in 17, 35 and 5 nodules, respectively. All 17 nodules with margin (+) and 13 of those with margin zero were assessed as having sufficient abalative margins on CT. The remaining 22 nodules with margin zero had insufficient margins on CT. The overall agreement between MRI and CT for the diagnosis of the ablative margin was moderate (κ=0.507, p<0.001). No local recurrence was found in 15 HCC nodules with margin (+), whereas local recurrence was found in 4 (11.8%) out of 34 HCC nodules with margin zero.
Conclusion: Administration of ferucarbotran before RFA enables the ablative margin to be visualised as a low-intensity rim, and also enables the evaluation of the ablative margin to be made earlier and more easily than with enhanced CT.

Received 30 July 2010
Revised 27 October 2010
Accepted 2 November 2010

DOI: 10.1259/bjr/64518148

Radiofrequency ablation (RFA) has become a widely used treatment for hepatocellular carcinoma (HCC) [1], with some studies reporting significant long-term survival results [2, 3]. One of the most difficult and troublesome issues in RFA is the lack of a reliable method for confirming that complete necrosis has been achieved in the treated lesion. CT and MRI are commonly used to evaluate the therapeutic response in the ablated tumours. The imaging hallmark of successful treatment is a lack of enhancement in the index tumour on CT or MRI [4, 5]. However, previous pathological examination has demonstrated the presence of micro-satellite nodules around the original tumour [6, 7]. Therefore, it is necessary to ablate liver parenchyma surrounding the original tumour, as well as the tumour itself, and the ablation zone of the surrounding normal tissue needs to be recognised.

Address correspondence to: Dr Masahiko Koda, Division of Medicine and Clinical Science, Department of Multidisciplinary Internal Medicine, Tottori University School of Medicine, 36-1 Nishicho, Yonago 683-8504, Japan. E-mail: masakoda@grape.med.tottori-u.ac.jp

In fact, several studies [8–10] have reported that the local recurrence rate in nodules with sufficient ablative margin is lower than that in those without sufficient ablative margin. The ablative margin is conventionally assessed by comparing enhanced CT images before and after RFA for HCC tumours.

Mori et al [11] reported a new method of evaluating the ablative margin using ferucarbotran (Resovist; Bayer Schering Pharma, Berlin, Germany), and demonstrated that the ablative margin is easily assessed by MRI. Ferucarbotran is a clinically approved superparamagnetic iron oxide (SPIO) that is liver specific on MRI. It is composed of SPIO microparticles (γ-Fe_2O_3) coated with carboxydextran. After intravenous administration, ferucarbotran is phagocytosed by Kupffer cells and equally distributed throughout the entire liver [12]. Kupffer cells are much more dominant in hepatic parenchyma than in cancer tissue. Therefore, the signal intensity from cancer in T_2* weighted sequences becomes relatively high compared with that from hepatic parenchyma. Ferucarbotran in ablated hepatic parenchyma would remain after ablation, showing low intensity around high-intensity cancer on post-ablational MR images.

The aim of this study was to determine the usefulness of ablative margin assessment by enhanced MRI using ferucarbotran administered before RFA in patients with liver cancer in comparison with post-ablation enhanced CT images after 1 month.

Methods and patients

From January 2008 to January 2009, we studied 42 consecutive patients with 55 HCCs and 3 patients with 5 metastatic liver cancers (2 originated from breast cancer, 2 from gastrointestinal stromal tumour and 1 from colon cancer) who were treated with percutaneous RFA at our hospital. The pre-operative clinical features of these 45 patients are listed in Table 1. Three patients with metastatic liver cancer had normal liver and 42 patients had underlying chronic liver disease: chronic hepatitis in 9 patients and cirrhosis in 33. The study was approved by the ethics committee of our institution (number 1186) and performed prospectively. The nature of the study was fully explained to the patients, and informed consent was obtained.

Prior to RFA, all patients underwent ultrasound, enhanced CT, enhanced MRI and/or CT scan under angiography. On enhanced CT or MRI, hyperenhancement in the arterial phase with washout in the portal phase was diagnosed as HCC. For each case of iso- or hypoenhancement in the arterial phase with hypoenhancement in the portal phase, diagnosis was obtained by percutaneous tumour biopsy. All metastatic liver cancers were diagnosed by percutaneous tumour biopsy.

We performed transcatheter arterial chemoembolisation (TACE) in 18 of 60 nodules prior to RFA. TACE was performed by selectively introducing a catheter into the segmental branch or subsegmental branch of the hepatic artery and injecting a mixture of an iodised oil and epirubicin hydrochloride (Farmorubicin; Pharmacia, Tokyo, Japan), followed by gelatin sponge (Gelpart; Astellas Pharma Inc., Tokyo, Japan).

Table 1. Baseline characteristics of the 45 patients (60 nodules)

Mean age (range), years	67.8±8.9	(51–85)
Male/female	35/10	
HCC	55 nodules	42 patients
Metastatic liver cancer	5 nodules	3 patients
Aetiology of HCC		
Hepatitis B	15 nodules	12 patients
Hepatitis C	31 nodules	24 patients
Hepatitis B+C	2 nodules	1 patient
Alcohol	4 nodules	3 patients
Cryptogenic	3 nodules	2 patients
Underlying liver disease		
Normal		3 patients
Chronic hepatitis		9 patients
Cirrhosis		33 patients
Pugh A		23 patients
Pugh B		10 patients
Tumour size (range), mm	16.8±5.9	(6.5–32.0)
Tumour number (range)	1.3±0.7	(1–4)
Combination of TACE	18 nodules	

HCC, hepatocellular carcinoma; TACE, transcatheter arterial chemoembolisation.

Study design

Ferucarbotran (0.016 ml kg^{-1} body weight) was injected intravenously 20–60 min before RFA. We performed MRI in all patients 7 days after RFA to evaluate the ablative margin. MRI was performed with a 1.5 T magnet (Magnetom Symphony; Siemens, Erlangen, Germany) using the following imaging protocol: T_2* weighted fast low-angle shot (FLASH); repetition time, 150–200 ms; echo time, 8.5 ms; flip angle, 60°; section thickness, 3 mm; bandwidth, 400 Hz per pixel.

For post-treatment evaluation, helical multiphasic CT examinations were performed 1 month after RFA using a 64 channel multidetector scanner (Aquilion 16; Toshiba Medical Systems, Tochigi, Japan) with the following imaging protocol: tube voltage, 120 kV; tube current, automatic mA setting; reconstruction section and interval thickness, 3 mm; detector configuration, 32×1 mm; pitch, 27; and gantry speed, 0.5 s per rotation. Unenhanced CT images were acquired, followed by triple-phase contrast-enhanced images during power injection of 100 ml of iopamidol (Iopamiron; Nihon-Schering, Osaka, Japan) at a rate of 2.7 ml s^{-1}. The entire liver was scanned three times. Early arterial phase imaging was initiated at 10 s, late arterial phase imaging at 20 s and portal venous phase imaging at 120 s after initiation of the injection. All scans were obtained with 3 mm slice pitch. Two patients with iodine hypersensitivity were evaluated by enhanced MRI rather than enhanced CT following RFA.

RFA protocol

RFA therapy was performed under sonographic guidance using a real-time convex scanner with 3.75 MHz probes (SSA-340A; Toshiba, Tokyo, Japan) and a biopsy guide device. We used two RFA systems: the RF3000 generator system on 40 nodules (67%) and the Cool-tip RF system (Radionics, Burlington, MA) on 20 nodules (33%).

In the RF3000 generator system, we used a 17 or 16 gauge expandable RFA device with 10 solid retractable curved electrodes with array diameters of 2–3.5 cm (LeVeen Needle Electrode; Boston Scientific Corporation, Natick, MA). The LeVeen needle was positioned in the tumour and the array was then expanded in three to five steps. The diameter of the array at each step was 10, 15, 20, 25, 30 and 35 mm. In the first step, hooks were deployed at an array diameter of 10 mm and RF power was initially applied at 30 W, which was increased by 10 W min^{-1} until it impeded out. The second step was begun at the RF power level reached in the first step, and RF power was increased by 10 W min^{-1} until it impeded out. This cycle was repeated at each step to full extension of the array. Additional ablation was applied at 70% of maximum power until it impeded out or for 15 min.

In the Cool-tip RF system, RF power was increased by 20 W min^{-1} from 40 W for a 3 cm exposed tip or 10 W min^{-1} from 30 W for a 2 cm exposed tip until maximum power was reached or it impeded out. After it impeded out three times, the power was decreased by 20 W for a 3 cm exposed tip or by 10 W for a 2 cm exposed tip and ablation was continued for 12 min.

Image analysis

MRI studies were reviewed on a computer workstation by two abdominal imaging radiologists (TK and ST, who had 12 and 11 years' experience, respectively). The reviewers knew the diagnosis of HCC or metastatic liver cancer but were blinded to other clinical data. Discrepancies between the two readers were resolved by discussion to reach consensus. On post-ablational MRI, we defined ablated surrounding hepatic parenchyma as a low-intensity rim around a central high-intensity area.

To evaluate whether the size of a high-intensity area on MRI agreed with the tumour size, we compared the tumour size on enhanced CT before treatment with the size of the high-intensity area on post-ablational MRI. The size was defined as the average of the major and minor axes; the size difference was measured for each tumour as the size of the high-intensity area on MRI minus the tumour size on enhanced CT.

We classified treatment efficacy on MRI into the following three grades (Figure 1). (1) Margin (+): a high-intensity area with a continuous low-intensity rim. The high-intensity area does not extend beyond the low-intensity rim, and a continuous rim is seen around the nodule on multidirectional MR images. (2) Margin zero: a high-intensity area with a discontinuous low-intensity rim. The high-intensity area does not extend beyond the rim, and the low-intensity rim is partially discontinuous. (3) Margin (−): the high-intensity area extends beyond the rim, with tumour protrusion.

We took tumour necrosis into account in defining treatment efficacy, using dynamic enhanced CT or MRI at 1 month after RFA. No residual tumour was defined as the absence of enhanced tumour areas, indicating complete tissue necrosis. The ablative margin was defined as ablated normal parenchyma surrounding the tumour, lying beyond the previously estimated tumour borders. Sufficient ablative margin was defined as the presence of ablative margin (at least 2 mm) on all sides of the tumour in all CT slices. Insufficient ablative margin was defined as the partial absence of the ablative margin.

Patients with HCC were followed up every 3 months with measurement of serum α-fetoprotein (normal $<12\,ng\,ml^{-1}$) and des-gamma-carboxyprothrombin (normal $<40\,mAU\,ml^{-1}$) levels, and enhanced CT or enhanced MRI. When recurrence was suspected, diagnosis of intrahepatic recurrence was made when there were positive findings in at least two of the following: CT, MRI, sonography, angiography and needle biopsy. Detection of local recurrence was defined as a recurrent tumour within or adjacent to the treated tumour.

Statistical analysis

The agreement between post-ablational MRI and enhanced CT for the diagnosis of the ablative margin was expressed by the κ coefficient (poor agreement, $\kappa=0$; slight agreement, $\kappa=0.21$–0.40; moderate agreement, $\kappa=0.41$–0.60; good agreement, $\kappa=0.61$–0.80; excellent agreement, $\kappa=0.81$–1.00). The Kaplan–Meier method was used to calculate the cumulative rate of local recurrence and the log-rank test was used for statistical analysis.

Results

Comparison between tumour size before treatment and the size of the high-intensity area on post-ablational MRI

We compared the tumour size on enhanced CT before treatment with the size of the high-intensity area on post-ablational MRI in 57 nodules, except for 3 nodules

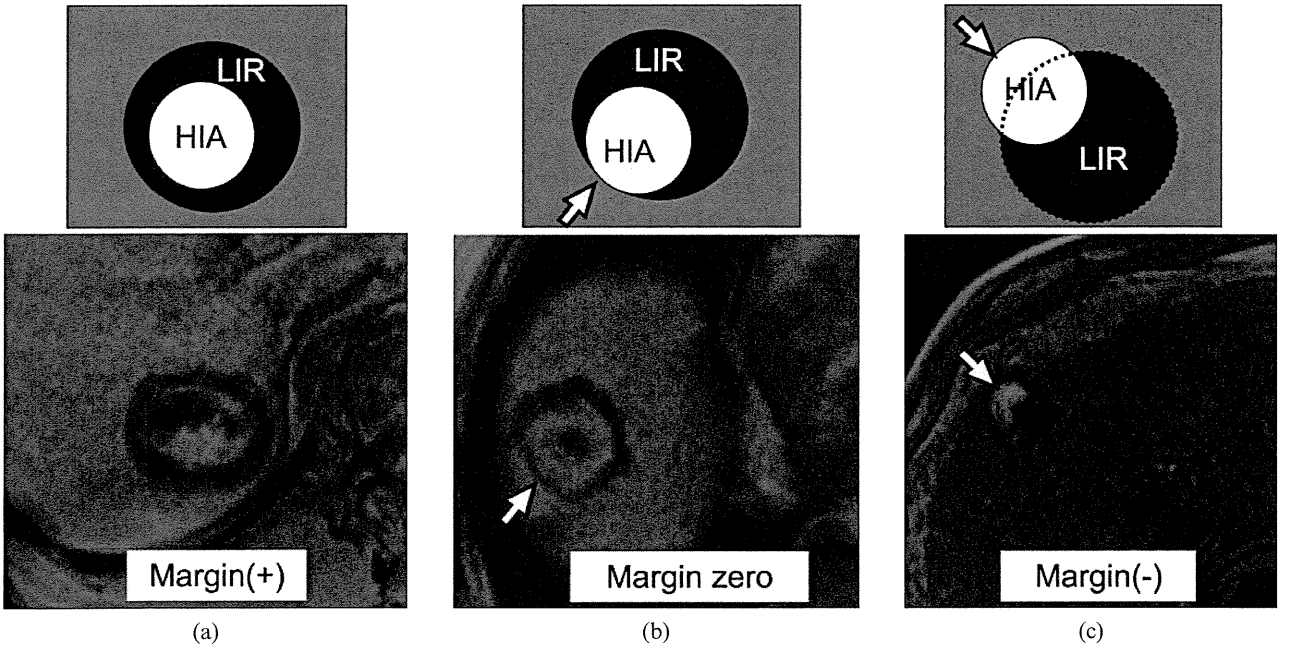

Figure 1. Grades of radiofrequency ablation treatment efficacy by post-ablational MRI. (a) Margin (+): high-intensity area (HIA) is contained within the low-intensity rim (LIR) and a continuous LIR is seen around the nodule. (b) Margin zero: HIA does not extend beyond the LIR, but the LIR is partially discontinuous (arrow). (c) Margin (−): discontinuous LIR with protrusion of HIA (arrow).

in which no high-intensity area was found. The size difference was within ±5 mm in 32 nodules (56.1%), within 5–10 mm in 13 (22.8%), within 10–15 mm in 11 (19.3%), and within 15–20 mm in 1 (1.8%) (Figure 2). Thus, the size of the high-intensity area on MRI was equal to or larger than the tumour size on enhanced CT. Figure 3 shows the presence of a high-intensity band on the outer side of an actual nodule on MRI after RFA. From these results, we consider that a high-intensity area seen after RFA consists of the tumour itself and a part of the ablated surrounding hepatic parenchyma.

Assessment of ablative margin on post-ablational MRI

We estimated the ablative margin of 60 nodules by MRI. Three nodules had no high-intensity area in the index tumours and were assessed as undeterminable. These three nodules were 10, 12 and 16 mm in size, and two nodules showed isoenhancement in the arterial phase with washout in the portal phase. Margin (−) was found in five nodules, two of which were retreated immediately. Of the remaining 52 nodules, 17 (32.7%) demonstrated margin (+) and 35 (67.3%) demonstrated margin zero; of these, 16 were located at the surface of the liver (Figure 4) and 2 were in contact with vessels.

Comparison of the assessment of ablative margin by post-ablational MRI with that by enhanced CT

Table 2 compares the ablative margin determined by MRI after 7 days with that by enhanced CT after 1 month. No nodule assessed as margin (+) or margin zero on MRI was assessed as having residual tumour on enhanced CT. All 17 nodules assessed as margin (+) on MRI were demonstrated as having sufficient ablative margin on enhanced CT. Of 35 nodules assessed as margin zero on MRI, 13 (37%) showed sufficient ablative margin and 22 (63%) showed insufficient ablative margin on enhanced CT. When enhanced CT is used as the gold standard, the sensitivity of MRI for sufficient margin was 56.7% (17/30) and the specificity was 100% (25/25). In one of three nodules assessed as margin (−) on MRI, enhanced CT after 1 month demonstrated local residue. The remaining two nodules were evaluated as having no residual tumour with insufficient ablative margin on enhanced CT (Figure 5). The overall agreement rate between post-ablational MRI and enhanced CT for the diagnosis of ablative margin was 73%. The κ coefficient was 0.507 ($p<0.001$), indicating moderate agreement.

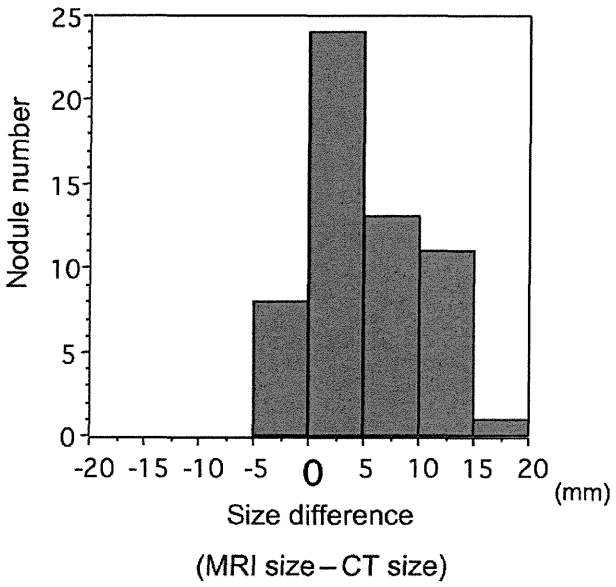

Figure 2. Frequency distribution of size difference (size of high-intensity area on post-ablational MRI minus the tumour size on pre-treatment enhanced CT).

Comparison of local recurrence rates in HCC nodules

During the observation periods (mean 20±5 months) after RFA in patients with HCC, local recurrence was detected in 4 (11.8%) of the 34 nodules that were assessed as margin zero; these nodules showed insufficient margin by enhanced CT and were retreated. No local recurrence was found in the 15 nodules assessed as margin (+). The cumulative detection rates of local recurrences were lower in the margin (+) nodules than in the margin zero nodules ($p=0.079$) (Figure 6).

Discussion

Treatment efficacy and ablative margin after RFA are conventionally evaluated by enhanced CT or MRI with dynamic study. Enhanced CT or MRI performed after RFA have some limitations. First, early assessment may be flawed by vascular abnormalities related to inflammatory change or microsurgical fistula. A thin rim of enhancement may be seen at the early stage, which is transient and commonly resolves over subsequent follow-up examinations [5, 13]. This area of benign periablational enhancement is likely to be due to inflammation and hyperaemia, may last nearly 1 month in some cases, and usually measures 1–2 mm in thickness, but may approach 5 mm. It is difficult to distinguish this appearance from residual tumour enhancement [14]; therefore, we perform enhanced CT at least 1 month after treatment, thus delaying the identification of treatment failure.

Second, the ablative margin is measured by comparing pre- and post-enhanced CT/MRI images by superimposition of hepatic anatomic landmarks; however, it is not easy to measure the acquired ablative margin because pre- and post-CT cross-sectional images are not perfectly reproducible. Nishijima et al [15] reported on the measurement of the ablative margin using iodised oil accumulation within HCCs as an index of HCC. The advantage of this method is to enable evaluation of both the ablative area and the index tumour on identical images, but it has two limitations: it requires arterial infusion of iodised oil prior to RFA, and iodised oil accumulation does not always reflect tumour size. Contrast-enhanced ultrasound can evaluate loss of

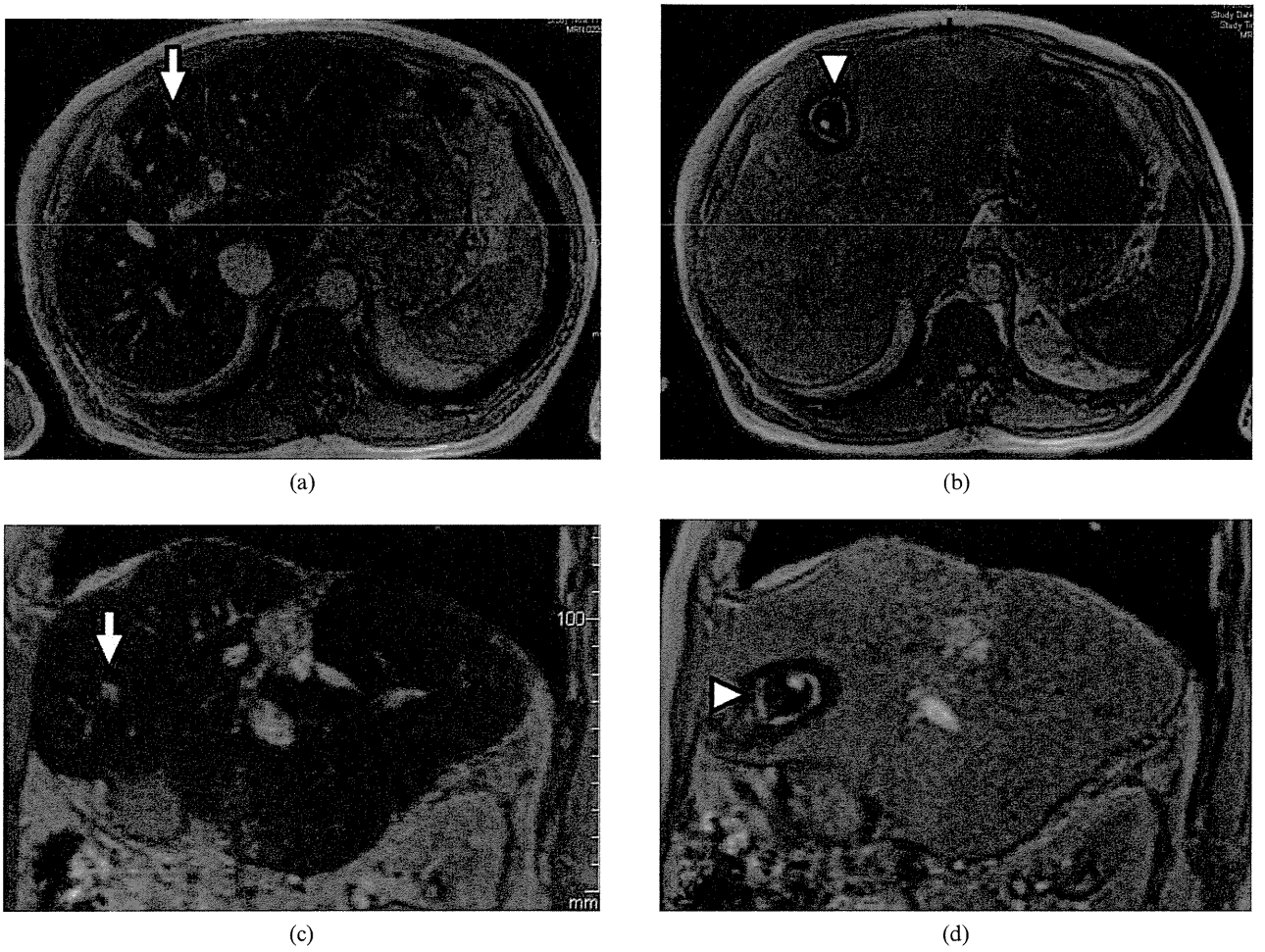

(a) (b)

(c) (d)

Figure 3. A 72-year-old male with an 8 mm hepatocellular carcinoma in liver segment V. (a) Transverse plane and (b) sagittal plane ferucarbotran-enhanced MRI before radiofrequency ablation (RFA) demonstrates a high-intensity tumour (arrow). (c) Transverse plane and (d) sagittal plane MRI after RFA shows three layers (low–high–low) around the index tumour. Part of the ablative margin was demonstrated to have become a high-intensity band (arrowhead).

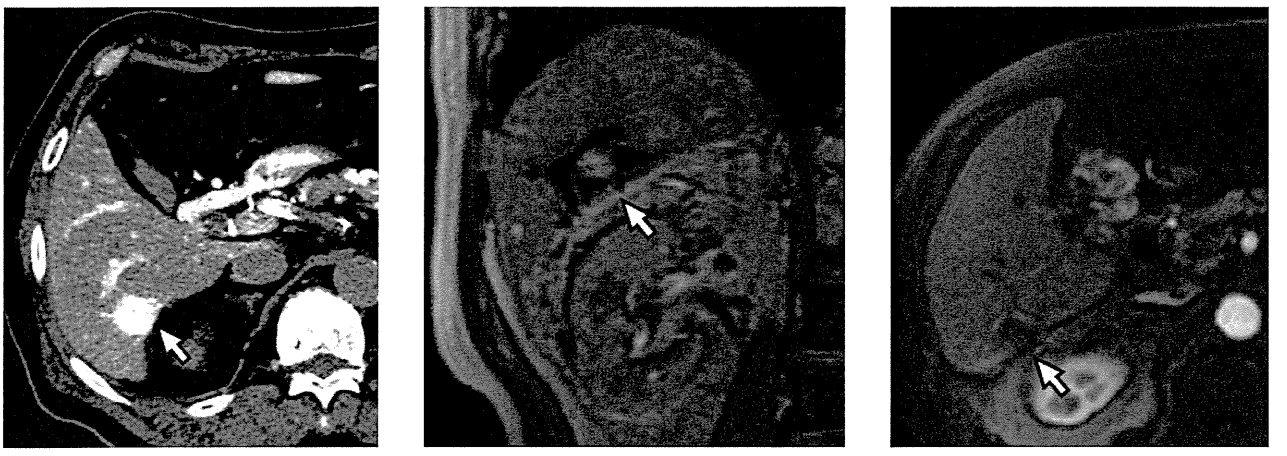

(a) (b) (c)

Figure 4. A 71-year-old male with a 21 mm hepatocellular carcinoma in liver segment VI. (a) Enhanced CT (arterial phase) reveals a hypervascular tumour (arrow). (b) Post-ablational MRI (coronal plane) reveals interruption of the rim at the liver surface (arrow). This tumour was evaluated as margin zero. (c) Enhanced MRI (arterial phase) 1 month after radiofrequency ablation reveals no hypervascular area (arrow). This tumour was evaluated as having no residue with insufficient ablative margin.

Table 2. Comparison of ablative margin by post-ablational MRI with that by enhanced CT

			Ferucarbotran-enhanced MRI			
			Margin (+)	Margin zero	Margin (−)	Total
Enhanced CT	No residual tumour	Sufficient margin	17	13	0	30
		Insufficient margin	0	22	2	24
	Residual tumour		0	0	1	1
	Total		17	35	3	55

Except for two nodules which were evaluated as tumour residue and treated by radiofrequency ablation before CT examination.

tumour stain and detect residual HCC, as in dynamic CT, but cannot confirm the presence of an ablative margin because contrast-enhanced ultrasound in most cases cannot distinguish tumour from ablated areas [16, 17].

Mori et al [11] have proposed a new method with ferucarbotran to assess the ablative margin. Ferucarbotran, which is administered intravenously, is phagocytosed by Kupffer cells. The signal from liver parenchyma in T_2* weighted sequences markedly decreased on MRI [18]. The number of Kupffer cells in cancerous tissues is significantly lower than in liver parenchyma, and decreases with decreasing histological grade [19]. Imai et al [20] demonstrated that ferucarbotran-enhanced MRI reflects Kupffer cell numbers in HCCs and dysplastic nodules; therefore, HCC is imaged as an area of high intensity within low-intensity liver.

Mori et al [11] demonstrated that the ablative margin appears as a low-intensity rim surrounding a high-intensity area including a tumour by administration of ferucarbotran prior to RFA. In the present study, we confirmed that a low-intensity rim is visualised around an ablated tumour. We compared the size of the high-intensity area on post-ablational MRI and the tumour size on pre-treatment enhanced CT in all tumours except for three nodules without any high-intensity area and found that the size of the high-intensity area on MRI was approximately equal to or larger than the actual tumour size on CT. We cannot explain why the high-intensity area on MRI after RFA was larger than the tumour size on enhanced CT in some cases. One possibility is that the degree of ablation may alter the signal intensity on MRI. In fact, a high-intensity band around a tumour was found, as shown in Figure 3. Because the magnetic susceptibility effect of ferucarbotran observed on MRI depends on cluster size [21], alterations in the signal intensity may result when the cluster size is changed by the extent of ablation. These findings indicate that the acquired ablative margin is larger than the low-intensity rim on MRI.

No areas of high intensity were seen in the ablated area of three nodules, although enhanced CT confirmed that these tumours had been completely ablated. The absence of a high-intensity area may be caused by these tumours having the same number of Kupffer cells as surrounding liver tissue. In fact, some well-differentiated HCCs are reported to contain as many Kupffer cells as surrounding liver tissue [20]. Because these three nodules were small and two nodules were isoenhanced in the arterial phase, it is highly possible that they are well-differentiated HCCs; however, we cannot confirm this finding because we did not examine ferucarbotran-enhanced MRI before RFA in these cases.

We compared the ablative margin on post-ablational MRI with that on enhanced CT. All nodules assessed as margin (+) or margin zero on MRI were demonstrated as having no residual tumour on enhanced CT. All nodules of margin (+) and 37% of those of margin zero had sufficient ablative margin on enhanced CT. The sensitivity of MRI for sufficient margin was 56.7%, while the specificity for sufficient margin was 100%. Furthermore,

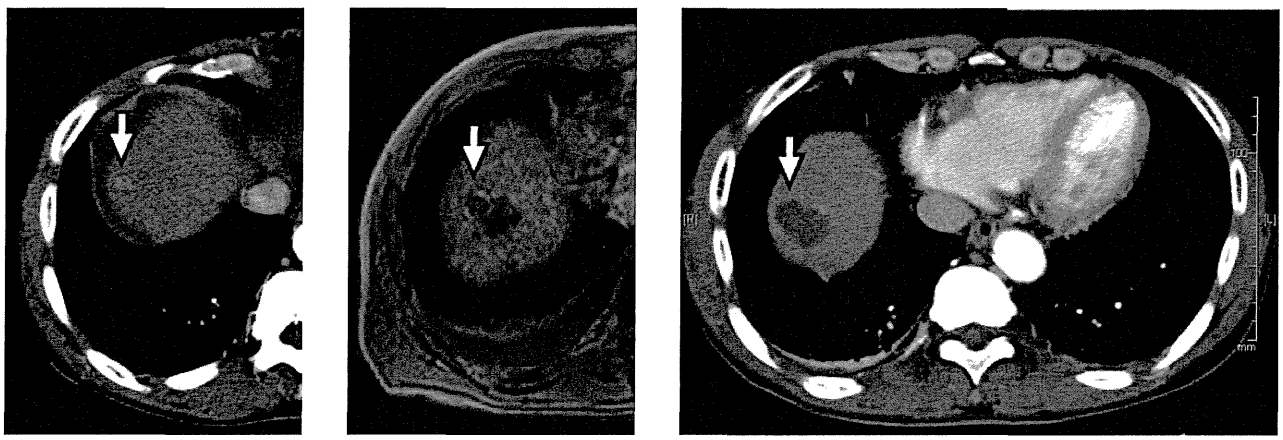

(a) (b) (c)

Figure 5. A 65-year-old male with a 12 mm hepatocellular carcinoma in liver segment VIII. (a) Enhanced CT (arterial phase) reveals a hypervascular tumour (arrow). (b) Post-ablational MRI demonstrates obvious discontinuity of the low-intensity rim with tumour protrusion [margin (−)] (arrow). (c) Enhanced CT (arterial phase) 1 month after radiofrequency ablation reveals no residue with insufficient ablative margin.

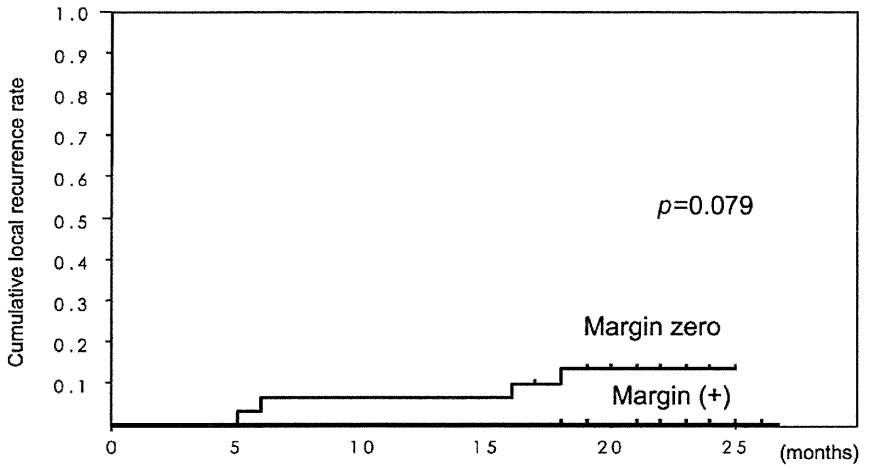

Figure 6. Comparison of the detection rates of local recurrences between the margin (+) nodules and the margin zero nodules on post-ablational MRI. It tended to be lower in margin (+) nodules than in the margin zero nodules (p=0.079).

the overall agreement between post-ablational MRI and enhanced CT for the diagnosis of ablative margin was moderate (κ=0.507). MRI may provide more accurate criteria for the assessment of the ablative margin than enhanced CT because MRI using ferucarbotran enables both the ablative margin and the index tumour to be visualised in the same image. At the least, margin (+) on MRI is a sufficient condition for sufficient ablative margin.

We classified 16 nodules located at the liver surface as margin zero; in these cases, the ablative margin could not be acquired anatomically at the surface site. A recent study found no difference in local tumour progression, distant intra- and extrahepatic tumour recurrence or major complication rate between tumours on the surface and those beneath the surface of the liver [22]. Therefore, we consider that the lack of an ablative margin in tumours located on the surface has no bearing on treatment efficacy. If these nodules are evaluated as having sufficient ablative margin, 33 nodules should be classified as margin (+) on MRI and sufficient margin on CT, and 6 nodules should be classified as margin zero on MRI and insufficient margin on CT.

We also classified two nodules in contact with large vessels as margin zero. The heat sink effect that occurs when a large vessel (>3 mm in diameter) abuts a tumour becomes an obstacle to achieving complete ablation [23]. Furthermore, the presence of large abutting vessels is a high-risk factor for major complications such as a biliary stenosis and portal thrombus [24]. We consider, therefore, that nodules in contact with large vessels should be classified as margin zero.

Of three nodules assessed as margin (−) on MRI, two were evaluated as having no residual tumour with insufficient margin on enhanced CT. As shown in Figure 5, although MRI showed that the index nodule lay beyond the ablated area, enhanced CT revealed that the area including the index nodule had become an avascular lesion. It is possible that projecting portions should also be considered ablated because of the so-called oven effect [25]. In essence, this effect involves the capsule of the tumour or cirrhotic tissue surrounding the tumour behaving as a thermal insulator, increasing heat retention within the tumour. Because ferucarbotran-enhanced MRI cannot distinguish between viable and non-viable HCC, we could not evaluate the viability of a portion projecting beyond the low-intensity rim on MRI.

We attempted to investigate the local recurrence rate in HCC nodules without residual tumours (margin (+) and margin zero). The cumulative detection rates of local recurrences were lower in the margin (+) nodules than in the margin zero nodules (p=0.079), although the difference was not significant statistically because of the small numbers of nodules. In particular, no local recurrence was found in the margin (+) nodules. Longer observation periods and larger numbers of nodules are necessary to evaluate local recurrence rates.

From these results, we recommend the following. Patients evaluated as margin (+) on post-ablational MRI have been treated completely. Patients with margin zero and margin (−) should undergo enhanced CT and, if a sufficient ablative margin is obtained, treatment has been successful. If an insufficient ablative margin and/or tumour residues are found, retreatment is required.

In conclusion, MRI using ferucarbotran is an easily performed, helpful method of evaluating the ablative margin in RFA. Further study with a large number of patients and long-term observation is needed to investigate its usefulness for predicting the occurrence of residual or recurrent tumours after RFA.

References

1. Schwarz RE, Smith DD. Trends in local therapy for hepatocellular carcinoma and survival outcomes in the US population. Am J Surg 2008;195:829–36.
2. Garrean S, Hering J, Saied A, Helton WS, Espat NJ. Radiofrequency ablation of primary and metastatic liver tumors: a critical review of the literature. Am J Surg 2008;195:508–20.
3. Ng KK, Poon RT, Lo C-M, Yuen J, Tso WK, Fan S-T. Analysis of recurrence pattern and its influence on survival outcome after radiofrequency ablation of hepatocellular carcinoma. J Gastrointest Surg 2008;12:183–91.
4. Vossen JA, Buijs M, Kamel IR. Assessment of tumor response on MR imaging after locoregional therapy. Tech Vasc Intervent Radiol 2006;9:125–32.
5. Park M-H, Rhim H, Kim Y-S, Choi D, Lim HK, Lee WF. Spectrum of CT findings after radiofrequency ablation of hepatic tumors. Radiographics 2008;28:379–92.
6. Okusaka T, Okada S, Ueno H, Ikeda M, Shimada K, Yamamoto J, et al. Satellite lesions in patients with small hepatocellular carcinoma with reference to clinicopathological features. Cancer 2002;95:1931–7.
7. Ikeda K, Seki T, Umehara H, Inokuchi R, Tamai T, Sakaida N, et al. Clinicopathological study of small hepatocellular

carcinoma with microscopic satellite nodules to determine the extent of tumor ablation by local therapy. Int J Oncol 2007;31:485–91.
8. Mulier S, Ni Y, Jamart J, Ruers T, Marchal G, Michel L. Local recurrence after hepatic radiofrequency coagulation. Multivariate meta-analysis and review of contributing factors. Ann Surg 2005;242:158–71.
9. Zytoon AA, Ishii H, Murakami K, El-Kholy MR, Furuse J, El-Dorry A, et al. Recurrence-free survival after radiofrequency ablation of hepatocellular carcinoma. A registry report of the impact of risk factors on outcome. Jpn J Clin Oncol 2007;37:658–72.
10. Peng Z-W, Zhang Y-J, Chen M-S, Liang H-H, Li J-Q, Zhang Y-Q, et al. Risk factors of survival after percutaneous radiofrequency ablation of hepatocellular carcinoma. Surg Oncol 2008;17:23–31.
11. Mori K, Fukuda K, Asaoka H, Ueda T, Kunimatsu A, Okamoto Y, et al. Radiofrequency ablation of the liver: determination of ablative margin at MR imaging with impaired clearance of ferucarbotran-feasibility study. Radiology 2009;251:557–65.
12. Stark DD, Weissleder R, Elizondo G, Hahn PF, Saini S, Todd LE, et al. Superparamagnetic iron oxide: clinical application as a contrast agent for MR imaging of the liver. Radiology 1988;168:297–301.
13. Tsuda M, Majima K, Yamada T, Saitou H, Ishibashi T, Takahashi S. Hepatocellular carcinoma after radiofrequency ablation therapy dynamic CT evaluation of treatment. J Clin Imaging 2001;25:409–15.
14. Smith S, Gillams A. Imaging appearances following thermal ablation. Clin Radiol 2008;63:1–11.
15. Nishijima N, Ohsaki Y, Kita R, Esoh Y, Yamanaka S, Kawakami H, et al. Proposal of the radicality grading as a criterion for therapeutic effectiveness of RFA against hepatocellular carcinoma, in relation to the local recurrence rate. Kanzo 2008;49:192–9.
16. Wen YL, Kudo M, Zheng RQ, Minami Y, Chung H, Suetomi Y, et al. Radiofrequency ablation of hepatocellular carcinoma: therapeutic response using contrast-enhanced coded phase-inversion harmonic sonography. AJR Am J Roentgenol 2003;181:57–63.
17. Koda M, Mandai M, Matono T, Sugihara T, Nagahara T, Ueki M, et al. Assessment of the ablated area after radiofrequency ablation by contrast-enhanced sonography: comparison with virtual sonography with magnetic navigation. Clin Imaging 2010;34:60–4.
18. Hamm B, Staks T, Taupitz M, Maibauer R, Speidel A, Huppertz A, et al. Contrast-enhanced MR imaging of liver and spleen: first experience in humans with a new superparamagnetic iron oxide. J Magn Reson Imaging 1994;4: 659–68.
19. Liu K, He X, Lei X-Z, Zhao L-S, Tang H, Liu L, et al. Pathomorphological study on location and distribution of Kupffer cells in hepatocellular carcinoma. World J Gastroenterol 2003;9:1946–9.
20. Imai Y, Murakami T, Yoshida S, Nishikawa M, Ohsawa M, Tokunaga K, et al. Superparamagnetic iron oxide-enhanced magnetic resonance images of hepatocellular carcinoma: correlation with histological grading. Hepatology 2000;32: 205–12.
21. Tanimoto A, Oshio K, Suematsu M, Pouliquen D, Stark DD. Relaxation effects of clustered particles. J Magn Reson Imaging 2001;14:72–7.
22. Sartori S, Tombesi P, Macario F, Nielsen I, Tassinari D, Catellani M, et al. Subcapsular liver tumors treated with percutaneous radiofrequency ablation: a prospective comparison with nonsubcapsular liver tumors for safety and effectiveness. Radiology 2008;248:670–9.
23. Kim Y-S, Rhim H, Cho OK, Koh BH, Kim Y. Intrahepatic recurrence after percutaneous radiofrequency ablation of hepatocellular carcinoma: analysis of the pattern and risk factors. Eur J Radiol 2006;59:432–41.
24. Rhim H, Lim HK, Kim Y-S, Choi D, Lee WJ. Radiofrequency ablation of hepatic tumors: lessons learned from 3000 procedures. J Gastroenterol Hepatol 2008;23:1492–500.
25. Livraghi T, Goldberg SN, Meloni F, Solbiati L, Gazelle GS. Hepatocellular carcinoma: comparison of efficacy between percutaneous ethanol injection and radiofrequency. Radiology 1999;210:655–63.

J Gastroenterol
DOI 10.1007/s00535-012-0641-9

ORIGINAL ARTICLE—LIVER, PANCREAS, AND BILIARY TRACT

Inhibition of hepatocellular carcinoma by PegIFNα-2a in patients with chronic hepatitis C: a nationwide multicenter cooperative study

Namiki Izumi · Yasuhiro Asahina · Masayuki Kurosaki · Gotaro Yamada · Tsutomu Kawai · Eiji Kajiwara · Yukishige Okamura · Takayuki Takeuchi · Osamu Yokosuka · Kazuya Kariyama · Joji Toyoda · Mie Inao · Eiji Tanaka · Hisataka Moriwaki · Hiroshi Adachi · Shinji Katsushima · Masatoshi Kudo · Kouichi Takaguchi · Yoichi Hiasa · Kazuaki Chayama · Hiroshi Yatsuhashi · Makoto Oketani · Hiromitsu Kumada

Received: 23 April 2012 / Accepted: 25 June 2012

Abstract
Background We investigated whether the administration of maintenance doses of interferon prevented hepatocellular carcinoma (HCC) in patients with chronic hepatitis C.
Methods Study 1: A multicenter, retrospective, cooperative study was carried out to determine whether long-term administration of low-dose peginterferon alpha-2a (PegIFNα-2a) prevented HCC development in patients with chronic hepatitis C. In total, 594 chronic hepatitis C patients without a history of HCC were enrolled and treated with 90 μg PegIFNα-2a administered weekly or bi-weekly for at least 1 year. Study 2: HCC developed in 16 of 99 additional patients without PegIFNα-2a treatment during 3.8 years of observation. A propensity-matched control study was then carried out to compare the incidence of

N. Izumi (✉) · Y. Asahina · M. Kurosaki
Department of Gastroenterology and Hepatology, Musashino Red-Cross Hospital, Musashino, Japan
e-mail: nizumi@musashino.jrc.or.jp

G. Yamada
Department of Internal Medicine, Kawasaki Hospital of Kawasaki Medical University, Okayama, Japan

T. Kawai
Department of Gastroenterology, Kanbara General Hospital, Fuji, Japan

E. Kajiwara
Department of Gastroenterology, Shinnittetsu Yahata Memorial Hospital, Kitakyushu, Japan

Y. Okamura
Department of Gastroenterology, Sano Kousei Hospital, Kitakyushu, Japan

T. Takeuchi
Department of Gastroenterology, Notogawa Hospital, Higashioumi, Japan

O. Yokosuka
Department of Gastroenterology and Hepatology, Chiba University, Chiba, Japan

K. Kariyama
Department of Hepatology, Okayama Citizens' Hospital, Okayama, Japan

J. Toyoda
Department of Gastroenterology and Hepatology, Sapporo Kousei Hospital, Sapporo, Japan

M. Inao
Department of Gastroenterology and Hepatology, Saitama Medical University, Moroyama, Japan

E. Tanaka
Second Department of Internal Medicine, Shinshu University, Matsumoto, Japan

H. Moriwaki
Department of Gastroenterology and Hepatology, Gifu University, Gifu, Japan

H. Adachi
Department of Hepatology, Tonami General Hospital, Tonami, Japan

S. Katsushima
Department of Gastroenterology, Kyoto Medical Center, Kyoto, Japan

M. Kudo
Department of Gastroenterology and Hepatology, Kinki University, Higashiosaka, Japan

K. Takaguchi
Department of Gastroenterology, Kagawa Central Hospital, Takamatsu, Japan

Published online: 09 August 2012

HCC between the 59 patients who received low-dose PegIFNα-2a (PegIFNα-2a group) and 59 patients who did not receive PegIFNα-2a treatment (control group), matched for sex, age, platelet count, and total bilirubin levels.

Results Study 1: HCC developed in 49 patients. The risk of HCC was lower in patients with undetectable hepatitis C virus RNA, ≤40 IU/L alanine aminotransferase (ALT), or ≤10 ng/L alpha-fetoprotein (AFP) 24 weeks after the start of therapy. Study 2: The incidence of HCC was significantly lower in the PegIFNα-2a group than in the control group.

Conclusions Low-dose and long-term maintenance administration of PegIFNα-2a decreased the incidence of HCC in patients with normalized ALT and AFP levels at 24 weeks compared with patients without normal ALT and AFP levels.

Keywords Chronic hepatitis C · Hepatocellular carcinoma · Peginterferon

Introduction

Hepatocellular carcinoma (HCC), the sixth most common cancer worldwide, often develops because of long-term hepatitis B or C virus infection [1, 2]. In particular, chronic hepatitis C and hepatic cirrhosis increase the risk of HCC; the annual incidence of tumor development in such patients may be as high as 2–4 % [3–5]. The incidence of HCC decreases in patients who achieve a sustained virological response (SVR) to interferon (IFN) treatment, although the incidence remains high in non-SVR patients [6–9]. A detailed analysis of HCC development revealed that chronic hepatitis C patients aged 65 years or more, especially those with advanced fibrosis of the liver, were at an increased risk of developing HCC [10]. For patients 65 years or older with advanced liver fibrosis, the dose of ribavirin is often reduced or the agent is discontinued, resulting in lower SVR rates in those with discontinuation of ribavirin. Establishing an effective treatment strategy for preventing the development of HCC is important for these high-risk patients.

Factors related to the development of HCC have been analyzed in patients who did not achieve an SVR even after IFN treatment; advanced fibrosis of the liver and high levels of serum alanine aminotransferase (ALT), and alpha-fetoprotein (AFP) are risk factors for HCC development [11, 12]. A randomized controlled trial was conducted in Western countries to determine whether combined peginterferon and ribavirin treatment with weekly administration of 90 μg peginterferon alpha-2a (PegIFNα-2a) could prevent HCC in non-responders. A 3.5-year follow up showed that administration of a maintenance dose of PegIFNα-2a did not reduce tumor incidence in these patients [13]. However, after 8.5 years of observation, the incidence of HCC was decreased among those in the PegIFNα-2a group with cirrhosis [14]. Meanwhile, Bruix et al. [15] reported that maintenance therapy with PegIFNα-2b did not prevent HCC in chronic hepatitis C patients with cirrhosis. In Japan, long-term low-dose administration of natural IFN has been reported to decrease the incidence of HCC [16]. In light of these conflicting results, investigations should be carried out in a large number of patients with chronic hepatitis C to resolve the question of whether IFN treatment prevents the development of HCC.

We carried out a multicenter retrospective cooperative study of patients with chronic hepatitis C to determine whether those treated with 90 μg PegIFNα-2a without ribavirin had a reduced incidence of HCC compared with those not treated with IFN.

Patients and methods

Study 1: analysis of risk factors for HCC in patients treated with long-term low-dose-PegIFNα-2a

In total, at 21 hepatitis centers throughout Japan, 743 patients with hepatitis C who had received 90 μg of PegIFNα-2a therapy weekly or bi-weekly for 1 year or more without having received the full dose (180 μg) since December 2003 were examined retrospectively for the development of HCC. The end of enrollment in this study was the end of December 2008 and the end of follow up was the end of December 2010. Patients with a history of HCC before the start of therapy and those with a therapy period of less than 48 weeks were excluded, leaving 594 patients who had undergone long-term administration of PegIFNα-2a for analysis. At the 21 centers involved in this

Y. Hiasa
Department of Gastroenterology and Hepatology, Ehime University, Matsuyama, Japan

K. Chayama
Department of Gastroenterology and Hepatology, Hiroshima University, Hiroshima, Japan

H. Yatsuhashi
Department of Gastroenterology and Hepatology, Nagasaki Medical Center, Nagasaki, Japan

M. Oketani
Department of Gastroenterology and Hepatology, Kagoshima University, Kagoshima, Japan

H. Kumada
Department of Hepatology, Toranomon Hospital, Tokyo, Japan

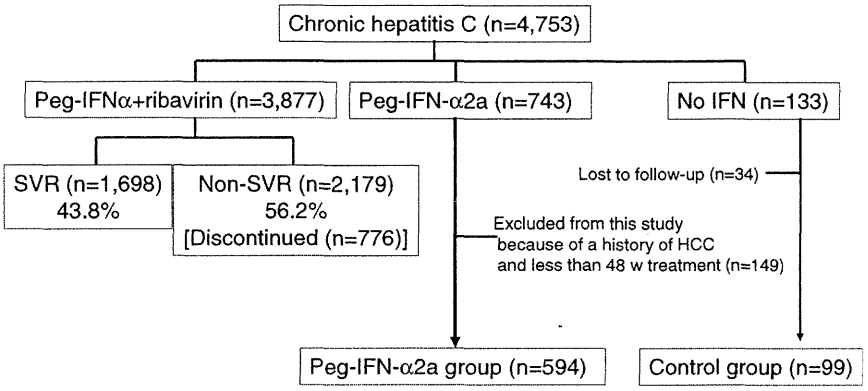

Fig. 1 Flow diagram of the patients' enrollment in the study. *Peg-IFNα* pegylated interferon α, *SVR* sustained viral response, *HCC* hepatocellular carcinoma, *w* week

study, 4,753 patients with chronic hepatitis C had been treated; Peg-IFN and ribavirin combination treatment had been administered to 3,877 patients, 743 patients had received Peg-IFN alone, and 133 patients had not agreed to receive IFN (a flow diagram of the enrollment of patients in this study is shown in Fig. 1). In the patients with Peg-IFN and ribavirin combination treatment, the SVR rate was 43.8 %; SVR was not achieved in 2,179 patients, and in 776 of these patients, the combination therapy was discontinued owing to adverse events or the patient's choice. Patients who failed to achieve an SVR were not included in this study, because the incidence of HCC is known to be reduced even in non-responders to IFN [17].

The backgrounds of the 594 patients studied are shown in Table 1. Findings from the liver biopsies of the patients were classified according to international standards [18]. Long-term PegIFNα-2a treatment is approved by the Japanese Medical Insurance system. Written informed consent was obtained from all patients prior to participation in this study. The study design was approved by the regional ethics committees of the 21 centers involved in this study, including the Musashino Red Cross Hospital, in accordance with the Helsinki Declaration. The 743 patients treated with PegIFNα-2a alone were not indicated for Peg-IFNα and ribavirin combination therapy because of anemia or heart disease. The 133 patients who did not agree to receive IFN served as the control group (see Fig. 1). A large proportion of the 594 study patients had advanced fibrosis of the liver and active inflammation. A dose of 90 μg PegIFNα-2a was administered to 512 and 82 patients weekly and biweekly, respectively, according to the patients' wishes. There were no significant differences between the weekly and biweekly groups in the patients' background data (data not shown).

The median duration of follow up in the PegIFNα-2a group was 1,273 days (range 228–2,768 days) and HCC was observed in 49 of the 594 patients (Table 1). Pretreatment and on-treatment factors associated with the development of HCC were analyzed by Student's *t*-test, the Mann–Whitney *U*-test, and the χ^2 test (Table 2). Independent factors for the development of HCC were assessed by multivariate analysis using logistic regression. The

Table 1 Background data of patients treated with PegIFNα-2a ($n = 594$)

	$n = 594$
Age (years)	61.7 ± 11.7
Sex (male/female)	258/336
BMI	23.2 ± 3.3
Genotype (1/2)	443/151
Diagnosis (ASC/CH/LC)	4/460/130
History of excess alcohol consumption (≥60 g/day; yes/no)	118/376
Fibrosis (F0, 1, 2/F3, 4)	443/151
Inflammatory activity (A0, 1/A2, 3)	469/125
Diabetes mellitus (no/yes)	499/95
LDL cholesterol (mg/dL)	94.2 ± 31.1
Fasting blood sugar (mg/dL)	106.3 ± 28.5
White blood cell count (/mm^3)	4,360 ± 1,470
Red blood cell count (×10^6/μL)	423.8 ± 56.4
Hemoglobin (g/dL)	13.3 ± 1.8
Platelet count (×10^3/μL)	137 ± 56
Albumin (g/dL)	4.0 ± 0.5
Total bilirubin (mg/dL)	0.8 ± 0.6
AST (IU/L)	65.8 ± 47.8
ALT (IU/L)	72.1 ± 68.0
Gamma-GTP (IU/L)	55.2 ± 51.3
Esophageal varices (no/yes)	344/31
Alpha fetoprotein (ng/L)	6.9 (4.2–13.8)
Once weekly or biweekly PegIFNα-2a	512:82
Baseline HCV RNA (KIU/mL)	1,024 (73–2,130)
Development of HCC (no/yes)	545/49

PegIFN pegylated interferon, *BMI* body mass index, *ASC* asymtomatic carrier, *CH* chronic hepatitis, *LC* liver cirrhosis, *LDL* low-density lipoprotein, *AST* aspartate aminotransferase, *ALT* alanine aminotransferase, *GTP* guanosine triphosphate, *HCV* hepatitis C virus, *HCC* hepatocellular carcinoma

Values are means ± SD, with ranges in parentheses

incidence of HCC was analyzed according to the ALT, AFP, and hepatitis C virus (HCV) RNA levels 24 weeks after the start of PegIFNα-2a administration by using the Kaplan–Meier method. The risk of HCC was analyzed, using the Kaplan–Meier method, only in the non-responders with detectable HCV RNA during PegIFNα-2a administration by dividing them according to the ALT and AFP levels 24 weeks after the start of therapy. The incidence of HCC was compared between the patients with ALT levels of <41 IU/L and those with levels of ≥41 IU/L, and between patients with serum AFP levels of <10 ng/L and those with levels of ≥10 ng/mL at 24 weeks after starting treatment, because at most of the centers participating in the this study, the upper normal range of serum ALT is set at 40 IU/L, and the most significant difference in the incidence of HCC was observed between the PegIFNα-2a and control group with the cut-off serum ALT set at 41 IU/L and cutoff serum AFP set at 10 ng/mL, 24 weeks after starting treatment. The HCV RNA level was measured using the Amplicor Monitor method with a lower detection limit of 50 IU/L (Roche Diagnostics, Tokyo, Japan). A history of excess alcohol consumption was determined as >60 g alcohol per day in order to exclude alcoholic liver disease.

An asymptomatic carrier was defined as a patient with a serum ALT level within the normal range and minimal inflammation or fibrosis in the biopsied tissues of the liver. Chronic hepatitis was defined as mild-to-severe fibrosis of the liver according to liver biopsy [18]. The diagnosis of liver cirrhosis was based on the results of histological examination of the biopsied liver tissues.

Study 2: incidence of HCC in the PegIFNα-2a therapy and non-administration (control) groups in comparison with propensity-matched controls

Ninety-nine of the 133 chronic hepatitis C patients who had not received IFN were examined as controls; patients in this group received liver-protective agents such as glycyrrhizin or were untreated, and the group was observed for more than 1 year. None of the individuals in the control groups had received IFN alone or PegIFNα and ribavirin combination treatment. They were treated for a median of 1,395 days (range 75–6,556 days). Fifty-nine of these patients underwent liver biopsy before the treatment and were considered the control group for the propensity-matched study. For the propensity-matched study, 59 patients were selected from the PegIFNα-2a group according to their age, sex, platelet count, and total bilirubin levels, which had been identified as independent pretreatment risk factors for the development of HCC in Study 1. The rates of HCC were analyzed using the Kaplan–Meier method, and the risk of HCC was analyzed particularly in patients with advanced fibrosis of the liver (F3 and F4).

Table 2 Comparison of HCC and non-HCC patients with long-term PegIFNα-2a administration ($n = 594$)

	Patients with or without development of HCC		p value
	With HCC ($n = 49$)	Without HCC ($n = 545$)	
Pretreatment parameters			
Age (years)	63.8 ± 1.7	61.3 ± 0.5	<0.05
Sex (male/female)	32/17	226/319	<0.01
BMI	24.0 ± 0.5	23.1 ± 0.2	n.s.
Genotype (1/2)	47/6	397/148	n.s.
History of excess alcohol consumption (≥60 g/day; yes/no)	11/38	107/338	n.s.
Fibrosis (F0, 1, 2/F3, 4)	25/24	418/127	<0.001
Inflammatory activity (A0, 1/A2, 3)	7/42	462/83	<0.001
Diabetes mellitus (no/yes)	38/11	461/84	n.s.
LDL cholesterol (mg/dL)	88.2 ± 9.0	94.7 ± 2.6	n.s.
White blood cell count (/mm^3)	4,355 ± 210	4,360 ± 64	n.s.
Red blood cell count (×10^6/μL)	420.8 ± 8.1	424.1 ± 2.6	n.s.
Hemoglobin (g/dL)	13.6 ± 0.3	13.3 ± 0.1	n.s.
Platelet count (×10^3/μL)	106 ± 8	140 ± 2	<0.001
Albumin (g/dL)	3.8 ± 0.1	4.0 ± 0.1	<0.001
Total bilirubin (mg/dL)	1.2 ± 0.1	0.8 ± 0.1	<0.001
AST (IU/L)	78.1 ± 6.8	64.6 ± 2.1	n.s.
ALT (IU/L)	72.8 ± 9.7	72.0 ± 2.9	n.s.
Gamma-GTP (IU/L)	68.7 ± 7.5	53.9 ± 2.3	n.s.
Alpha fetoprotein (ng/L)	17.1 (4.4–36.8)	16.7 (4.1–23.1)	n.s.
Esophageal varices	29.0 % (9/31)	6.4 % (22/344)	<0.01
On-treatment parameters			
ALT (IU/L)	59.4 ± 5.7	44.6 ± 1.8	<0.05
Alpha fetoprotein (ng/L)	9.8 (4.6–17.4)	5.5 (3.7–11.1)	<0.01
HCV RNA level (KIU/mL)	236 (<0.5–2,210)	21 (<0.5–1,780)	<0.05

n.s. not significant

Statistical analysis

Categorical data were compared using the χ^2 test or Fisher's exact test. The distributions of continuous variables were analyzed using Student's t-test and the Mann–Whitney U-test for two groups. Multivariate analysis was

conducted using logistic regression. The cumulative incidence curve was determined using the Kaplan–Meier method and differences between groups were assessed by the log-rank test. For all methods, the level of significance was set at $p < 0.05$. Multivariate analysis of the risk of HCC was carried out using the Cox proportional hazard model. Statistical analyses were performed using the Statistical Package for the Social Sciences software version 11.0 (SPSS, Chicago, IL, USA). In Study 1, age, sex, platelet count, and total bilirubin levels were identified as independent factors for the development of HCC; therefore, these factors were selected for the propensity-matched control study (Study 2) in which 59 patients from the PegIFNα-2a group were included.

Results

Study 1

We analyzed the factors involved in the development of HCC in patients who received 90 μg PegIFNα-2a weekly or biweekly for more than a year. The incidence of HCC did not differ significantly between the groups treated with PegIFNα-2a weekly and biweekly (34 of 512 vs. 15 of 82, respectively). As shown in Table 2, univariate analysis revealed statistically significant differences in the pretreatment parameters including age, sex, fibrosis of the liver, platelet count, albumin level, and total bilirubin, between patients who developed HCC and those who did not. Endoscopy was carried out in 375 patients, and esophageal varices were noted in 31 of them. The incidence of HCC was higher in patients with esophageal varices than in those without varices [29.0 % (9 of 31) vs. 6.4 % (22 of 344)]. Assessment of on-treatment factors by univariate analysis revealed statistically significant differences in serum ALT, AFP, and HCV RNA levels 24 weeks after the start of PegIFNα-2a maintenance treatment (Table 2).

Multivariate analysis including pretreatment parameters revealed that age, sex, fibrosis of the liver, platelet count, and total bilirubin were independent risk factors for HCC development (Table 3). Multivariate analysis including on-treatment parameters identified ALT levels of ≥41 IU/L and AFP levels of ≥10 ng/L 24 weeks after the start of the PegIFNα-2a therapy as independent risk factors for HCC development (Table 3).

The incidence of HCC was significantly lower in patients with ALT levels of ≤40 IU/L than in those with ALT levels of ≥41 IU/L 24 weeks after the start of observation (Fig. 2). The incidence of HCC was also significantly lower in patients with AFP concentrations of <10 ng/mL at 24 weeks after the start of observation than in those with AFP concentrations of ≥10 ng/mL (Fig. 3). The dose of PegIFNα-2a was reduced to 45 μg in 16 patients because of neutropenia and thrombocytopenia. In addition, PegIFNα-2a was discontinued in 18 patients because of adverse events, including depression (7 patients), interstitial pneumonitis (3 patients), thrombocytopenia (3 patients), neutropenia (1 patient), itching (1 patient), and ascites (3 patients). No statistically significant differences were found between the patients with reduced dosage or treatment interruption and those without treatment modifications with respect to overall survival, HCC incidence, ascites formation, variceal bleeding, hepatic encephalopathy, and 2-point increases in the Child-Pugh score. No patients underwent liver transplantation.

Table 3 Independent risk factors for HCC development in patients treated with 90 μg PegIFNα-2a weekly or bi-weekly, evaluated by multivariate analysis (logistic regression analysis)

	Multivariate analysis		
	Odds ratio	95 % Confidence interval (CI)	*p*
Age (years) (every 5 years)	2.24	1.76–9.33	<0.005
Sex (male/female)	3.16	1.56–10.7	<0.005
Fibrosis (F3, 4/F0, 1, 2)	1.69	1.18–5.2	<0.01
Platelet count (<120 × 10^3/μL vs. ≥120 × 10^3/μL)	3.24	1.44–27.6	<0.01
Total bilirubin (mg/dL)	1.59	1.09–2.58	<0.05
ALT (at 24 weeks) (≥41 vs. <40 IU/L)	2.49	1.51–8.28	<0.05
AFP (at 24 weeks) (≥10 vs. <10 ng/L)	3.78	1.92–11.8	<0.01

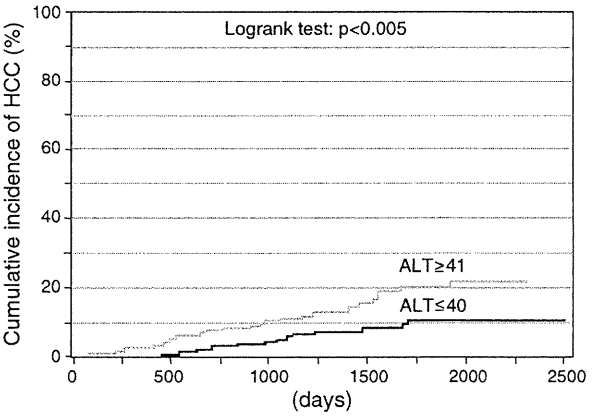

Fig. 2 Comparison of HCC rates in patients administered with PegIFNα-2a ($n = 594$) with respect to alanine aminotransferase (*ALT*) levels 24 weeks after the start of therapy. *Black line* patients with ALT ≥41 IU/L in the first 24 weeks, *gray line* patients with ALT ≤40 IU/L in the first 24 weeks

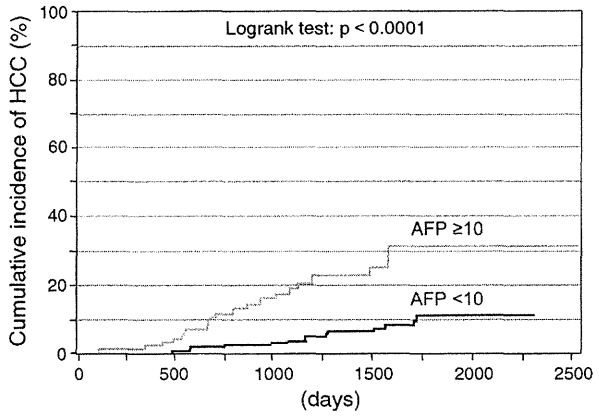

Fig. 3 Comparison of HCC rates in patients administered PegIFNα-2a ($n = 594$) with respect to alpha-fetoprotein (*AFP*) levels in the first 24 weeks after the start of therapy. *Black line* patients with AFP ≥10 ng/mL at 24 weeks, *gray line* patients with AFP <10 ng/mL at 24 weeks

Study 2

We compared the incidence of HCC between 59 patients in the control group and the same number of patients in the PegIFNα-2a group using the matched-pair test. The backgrounds of the patients are shown in Table 4. The PegIFNα-2a group had higher rates of advanced fibrosis (F3 and F4) and active inflammation (A2 and A3). No other differences were found between the two groups, except for the white blood cell count (Table 4).

Development of HCC was observed in 2 patients in the PegIFNα-2a group and 8 in the control group. The incidence of HCC was compared between the two groups, using the Kaplan–Meier method. The incidence of HCC in the PegIFNα-2a group was significantly lower than that in the control group (log-rank test, $p = 0.0187$; Fig. 4). Among the patients with advanced fibrosis of the liver (F3 and F4), those in the PegIFNα-2a group had a lower incidence of HCC than those in the control group. The independent risk factors for the development of HCC were analyzed using the stepwise Cox proportional hazard model. Only PegIFNα-2a administration and age were identified as independent risk factors for the development of HCC (Table 5).

Discussion

The number of HCC cases resulting from HCV infection continues to increase worldwide [19]. To date, IFN therapy is the most effective preventive measure against HCC in patients with chronic hepatitis C; furthermore, the incidence of HCC is reduced in patients who achieve an SVR to IFN [6–9] Therefore, achieving an SVR is the most effective approach for reducing the risk of developing HCC. In Japan, the incidence of HCC is elevated in older patients with hepatitis C. Corroborating this finding, the results of a Japanese study show a higher risk of HCC in patients aged 65 years and more [10]. Therefore, prevention of HCC in aged patients is an important challenge.

In the present multicenter, cooperative, retrospective study conducted in Japan, the incidence of HCC was reduced in patients who received 90 μg PegIFNα-2a weekly or biweekly and had AFP values of <10 ng/mL and ALT values of ≤40 IU/L 24 weeks after the start of the treatment. The results of the matched case–control study of the PegIFNα-2a group and the non-IFN control group show that the incidence of HCC was significantly lower in the PegIFNα-2a group than in the control group, especially in patients with advanced fibrosis of the liver (F3 and F4). However, there could have been a selection bias between

Table 4 Backgrounds of the patients in the propensity-matched control study (PegIFNα-2a group, $n = 59$; control group, $n = 59$)

	PegIFNα-2a group ($n = 59$)	Control group ($n = 59$)	p value
Age (years)	60.5 ± 13.0	63.3 ± 10.5	n.s.
Gender (male/female)	24/35	25/34	n.s.
BMI	22.9 ± 3.6	22.9 ± 3.4	n.s.
Genotype (1/2)	49/10	46/13	n.s.
History of excess alcohol consumption (60 g/day; yes/no)	10/49	4/55	n.s.
Fibrosis (F0, 1, 2/F3, 4)	37/22	43/16	<0.05
Development of HCC (F0–2/F3, 4)	1/1	1/7	n.s.
Inflammatory activity (A0,1/A2, 3)	19/40	30/29	<0.05
Diabetes mellitus (no/yes)	57/2	56/3	n.s.
LDL cholesterol (mg/dL)	95.3 ± 23.8	117.0 ± 4.2	n.s.
White blood cell count (/mm^3)	4,260 ± 1,239	5,193 ± 2,078	<0.05
Red blood cell count (×10^{-4}/μL)	430 ± 57.8	441 ± 44.9	n.s.
Hemoglobin (g/dL)	13.6 ± 1.5	13.6 ± 1.9	n.s.
Platelet count (×10^{-3}/μL)	14.5 ± 5.7	15.8 ± 5.7	n.s.
Albumin (g/dL)	4.1 ± 0.5	4.1 ± 0.4	n.s.
Total bilirubin (mg/dL)	0.7 ± 0.5	0.9 ± 0.7	n.s.
AST (IU/L)	58.3 ± 47.7	49.7 ± 26.6	n.s.
ALT (IU/L)	63.6 ± 68.7	58.0 ± 39.2	n.s.
Gamma-GTP (IU/L)	78.3 ± 81.3	55.3 ± 75.1	n.s.
Baseline alpha-fetoprotein (AFP) (ng/L)	7.2 (4.3–14.2)	7.7 (3.9–13.8)	n.s.
Baseline HCV RNA level (KIU/mL)	1,230 (24–3,870)	1,024 (38–3,110)	n.s.

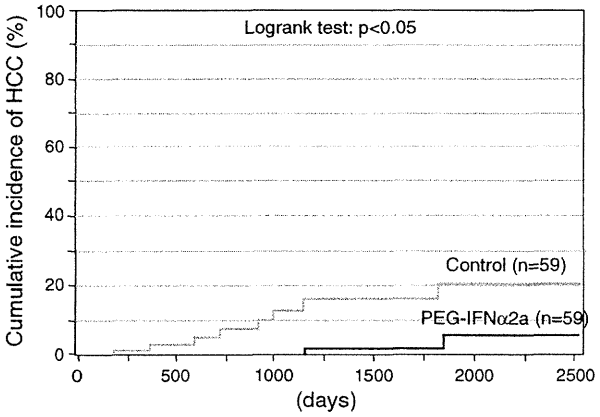

Fig. 4 Comparison of HCC rates between the long-term PegIFNα-2a administration group ($n = 59$) and non-administration group ($n = 59$) in the propensity-matched control study (Kaplan–Meier log-rank test, $p = 0.019$)

Table 5 Risk factors for HCC in the propensity-matched control study (Cox proportional hazard model)

Variables	Risk ratio	95 % CI	p value
PegIFN versus control	0.17	0.03–0.75	<0.05
Age (every 1 year)	1.12	1.02–1.25	<0.05
Fibrosis (F3, 4 vs. F0, 1, 2)	1.70	0.75–4.16	n.s.
Platelet count (every 10 × $10^3/\mu L$)	0.89	0.73–1.09	n.s.
Albumin (every 1.0 g/dL)	0.80	0.10–6.68	n.s.
On-treatment AFP (<10 vs. ≥10 ng/L)	4.07	0.59–40.12	n.s.

the PegIFNα-2a group and the control group (patients who did not agree to receive IFN treatment), because this was a retrospective and non-randomized study. However, concordant with the findings of the HALT-C study [14], the present results show that PegIFNα-2a inhibits the development of HCC in patients with advanced fibrosis of the liver.

Recent studies show that polymorphisms in the host *IL28B* gene are important factors in the response to PegIFNα and ribavirin combination therapy [20, 21]. However, the mechanism of IL28B involvement in the response to PegIFNα and ribavirin has not been elucidated completely. A recent report has shown that IL28B is a significant factor in the development of HCC as well as in the response to IFN therapy [22]. Further studies are warranted to analyze the relationship between IL28B and inhibition of the development of HCC by PegIFNα in chronic hepatitis C.

Risk factors for the development of HCC have been discussed previously. Increased intrahepatic fat is involved in the development of HCC in chronic hepatitis C patients [23, 24]. In addition, diabetes-associated fat disorder [25, 26], hepatic iron overload [27], advanced fibrosis, older age, and fatty deposits in the liver are risk factors for HCC development [4]. Therefore, it is important to establish strategies to mitigate these risk factors to prevent the development of HCC and thus improve the outcomes of hepatitis C patients.

IFN therapy after HCC treatment is reported to inhibit the recurrence of tumors [28, 29], and a meta-analysis has revealed a trend toward inhibition of the recurrence of HCC [30, 31]. The prevention of HCC is an important issue that needs to be addressed to improve the survival of chronic hepatitis C patients. The findings of the present study and the HALT-C trial [14] indicate the effectiveness of long-term administration of maintenance IFN for preventing the development of HCC in chronic hepatitis C patients without an SVR. Improvement in ALT levels is also known to be an important predictor for the prevention of HCC [32]. A low AFP value during IFN administration is also recognized as a significant indicator of a lower risk of HCC [33, 34]. Recently, Osaki et al. [35] reported that a decrease of serum AFP during treatment with IFN was associated with a reduced incidence of HCC. Taking these findings and our own together, we conclude that maintenance administration of low-dose PegIFNα-2a weekly or biweekly to non-SVR patients with chronic hepatitis C decreases the incidence of HCC, especially in patients whose serum ALT and AFP levels are within the normal range 24 weeks after the start of treatment. The preventive effects of IFN against the development of HCC without elimination of the virus may be associated with its anticarcinogenic effects [16, 35]; however, the precise mechanism should be investigated.

The limitations of the present study are that it is retrospective and multicentric; therefore, potentially there may have been a selection bias. However, the reduction of the rate of development of HCC by maintenance administration of PegIFNα-2a in the patients in whom serum ALT and AFP levels were within the normal ranges 24 weeks after the start of treatment may be attributable to the anticarcinogenic effects of IFN without elimination of the virus.

Conclusion

The incidence of HCC was lower in non-SVR patients with chronic hepatitis C who were administered with maintenance low-dose PegIFNα-2a; especially in those whose serum ALT and AFP levels were within the normal ranges 24 weeks after the start of treatment.

Acknowledgments This study was supported by a Grant-in-Aid from the Japanese Ministry of Health, Welfare, and Labor.

Conflict of interest Namiki Izumi received lecture fees from Chugai Co. and MSD Co. in 2011.

References

1. Parkin DM, Bray F, Ferlay J, Pisani P. Global cancer statistics, 2002. CA Cancer J Clin. 2005;55:74–108. doi:10.3322/canjclin.55.2.74.
2. Llovet JM, Burroughs A, Bruix J. Hepatocellular carcinoma. Lancet. 2003;362:1907–17. doi:10.1016/S0140-6736(03)14964-1.
3. Kiyosawa K, Sodeyama T, Tanaka E, Gibo Y, Yoshizawa K, Nakano K, et al. Interrelationship of blood transfusion, non-A, non-B hepatitis and hepatocellular carcinoma: analysis by detection of antibody to hepatitis C virus. Hepatology. 1990;12:671–5. doi:10.1002/hep.1840120409.
4. Namiki I, Nishiguchi S, Hino K, Suzuki F, Kumada H, Itoh T, et al. Management of hepatitis C; Report of the consensus meeting at the 45th annual meeting of the Japan Society of Hepatology (2009). Hepatol Res. 2010;40:347–68. doi:10.1111/j.1872-034X.2010.00642.x.
5. Tanaka Y, Hanada K, Mizokami M, Yeo AE, Shin JW, Gojobori T, et al. A comparison of the molecular clock of hepatitis C virus in the United States and Japan predicts that hepatocellular carcinoma incidence in the United States will increase over the next two decades. Proc Natl Acad Sci USA. 2002;99:11584–9. doi:10.1073/pnas.242608099.
6. Ikeda K, Saitoh S, Arase Y, Chayama K, Suzuki Y, Kobayashi M, et al. Effect of interferon therapy on hepatocellular carcinoma in patients with chronic hepatitis type C: a long-term observation study of 1,643 patients using statistical bias correction with proportional hazard analysis. Hepatology. 1999;29:1124–30.
7. Imai Y, Kawata S, Tamura S, Yabuuchi I, Noda S, Inada M, et al. Relation of interferon therapy and hepatocellular carcinoma in patients with chronic hepatitis C. Ann Intern Med. 1998;129:94–9.
8. Bruno S, Stroffolini T, Colombo M, Bollani S, Benveguu L, Mazzella G, et al. Sustained virological response to interferon-alpha is associated with improved outcome in HCV-related cirrhosis: a retrospective study. Hepatology. 2007;45:579–87. doi:10.1002/hep.21492.
9. Veldt BJ, Heathcote EJ, Wedemeyer H, Reichen J, Hofmann WP, Zeuzem S, et al. Sustained virological response and clinical outcomes in patients with chronic hepatitis C and advanced fibrosis. Ann Intern Med. 2007;147:677–84.
10. Asahina Y, Tsuchiya K, Tamaki N, Hirayama I, Tanaka T, Sato M, et al. Effect of aging on risk for hepatocellular carcinoma in chronic hepatitis C virus infection. Hepatology. 2010;52:518–27. doi:10.1002/hep.23691.
11. Amarapurkar D, Han KH, Chan HL, Ueno Y, Asia-Pacific working party on prevention of hepatocellular carcinoma. Application of surveillance programs for hepatocellular carcinoma in the Asia-Pacific Region. J Gastroenterol Hepatol. 2009;24:955–61. doi:10.1111/j.1440-1746.2009.05805.x.
12. Tamura Y, Yamagiwa S, Aoki Y, Kurita S, Suda T, Ohkoshi S, et al. Serum alpha-fetoprotein levels during and after interferon therapy and the development of hepatocellular carcinoma in patients with chronic hepatitis C. Dig Dis Sci. 2009;54:2530–7.
13. Di Bisceglie AM, Shiffman ML, Everson GT, Lindsay KL, Everhart JE, Wright EC, et al. Prolonged therapy of advanced chronic hepatitis C with low-dose peginterferon. N Engl J Med. 2008;359:2429–41. doi:10.1056/NEJMoa0707615.
14. Lok AS, Everhart JE, Wright EC, Di Bischeglie AM, Kim HY, Stering RK, et al. Maintenance peginterferon therapy and other factors associated with hepatocellular carcinoma in patients with advanced hepatitis C. Gastroenterology. 2011;140:840–9. doi:10.1053/j.gastro.2010.11.050.
15. Bruix J, Poynard T, Colombo M, Schiff E, Burak K, Heathcote EJ, et al. Maintenance therapy with peginterferon alfa-2b does not prevent hepatocellular carcinoma in cirrhotic patients with chronic hepatitis C. Gastroenterology. 2011;140:1990–9. doi:10.1053/j.gastro.2010.11.050.
16. Arase Y, Ikeda K, Suzuki F, Suzuki Y, Kobayashi M, Akuta N, et al. Prolonged-interferon therapy reduces hepatocarcinogenesis in aged-patients with chronic hepatitis C. J Med Virol. 2007;79:1095–102. doi:10.1002/jmv.20866.
17. Poynard T, Moussali J, Ratziu V, Regimberu C, Opolan P. Effects of interferon therapy in "non-responder" patients with chronic hepatitis C. J Hepatol. 1999;31S:178–83. doi:10.1016/S0168-8278(99)80397-3.
18. Desmet VJ, Gerber M, Hoofnagle JH, Manns M, Scheuer P. Classification of chronic hepatitis: diagnosis, grading and staging. Hepatology. 1994;19:1513–20. doi:10.1016/0270-9139(94)90250-X, doi:10.1002/hep.1840190629.
19. Kanwal F, Hoang T, Kramer JR, Asch SM, Goetz MB, Zeringue A, et al. Increasing prevalence of HCC and cirrhosis in patients with chronic hepatitis C virus infection. Gastroenterology. 2011;140:1182–8. doi:10.1053/j.gastro.2010.12.032.
20. Ge D, Fellay J, Thompson AJ, Simon JS, Shianna KV, Urban TJ, et al. Genetic variation in IL28B predicts hepatitis C treatment-induced viral clearance. Nature. 2009;461:399–401. doi:10.1038/nature08309.
21. Tanaka Y, Nishida N, Sugiyama M, Kurosaki M, Matsuura K, Sakamoto N, et al. Genome-wide association of IL28B with response to pegylated interferon-alpha and ribavirin therapy for chronic hepatitis C. Nature. 2009;41:1105–9.
22. Fabris C, Falleti E, Cussigh A, Bitetto D, Fontanini E, Bignulin S, et al. IL-28B rs 12979860 C/T allele distribution in patients with liver cirrhosis: role in the course of chronic viral hepatitis and the development of HCC. J Hepatol. 2011;54:716–22. doi:10.1016/j.jhep.2010.07.019.
23. Kurosaki M, Hosokawa T, Matsunaga K, Hirayama I, Tanaka T, Sato M, et al. Hepatic steatosis in chronic hepatitis C is a significant risk factor for developing hepatocellular carcinoma independent of age, sex, obesity, fibrosis stage and response to interferon therapy. Hepatol Res. 2010;40:870–7. doi:10.1111/j.1872-034X.2010.00692.x.
24. Koike K. Steatosis, liver injury, and hepatocarcinogenesis in hepatitis C viral infection. J Gastroenterol. 2009;44(Suppl 19):82–8. doi:10.1007/s00535-008-2276-4.
25. Veldt BJ, Chen W, Heathcote EJ, Wedemeyer H, Reichen J, Hofman WP, et al. Increased risk of hepatocellular carcinoma among patients with hepatitis C cirrhosis and diabetes mellitus. Hepatology. 2008;47:1856–62. doi:10.1002/hep.22251.
26. Lai MS, Hsieh MS, Chiu YH, Chen TH. Type 2 diabetes and hepatocellular carcinoma: a cohort study in high prevalence area of hepatitis virus infection. Hepatology. 2006;43:1295–302. doi:10.1002/hep.21208.
27. Furutani T, Hino K, Okuda M, Gondo T, Nishina S, Kitase A, et al. Hepatic iron overload induces hepatocellular carcinoma in transgenic mice expressing the hepatitis C virus polyprotein. Gastroenterology. 2006;130:2087–98. doi:10.1053/j.gastro.2006.02.060.
28. Kubo S, Nishiguchi S, Hirohashi K, Tanaka H, Shuto T, Kinoshita H. Randomized clinical trial of long-term outcome after resection of hepatitis C virus-related hepatocellular carcinoma by

postoperative interferon therapy. Br J Surg. 2002;89:418–22. doi: 10.1046/j.0007-1323.2001.02054.x.
29. Kudo M, Sakaguchi Y, Chung H, Hatanaka K, Hagiwara S, Ishikawa E, et al. Long-term interferon maintenance therapy improves survival in patients with HCV-related hepatocellular carcinoma after curative radiofrequency ablation. A matched case–control study. Oncology. 2007;72(Suppl 1):132–8. doi: 10.1159/000111719.
30. Singal AK, Freeman DH Jr, Anand BS. Meta-analysis: interferon improves outcomes following ablation or resection of hepatocellular carcinoma. Aliment Pharmacol Ther. 2010;32:851–8. doi:10.1111/j.1365-2036.2010.04414.x.
31. Miyake Y, Takaki A, Iwasaki Y, Yamamoto K. Meta-analysis: interferon-alpha prevents the recurrence after curative treatment of hepatitis C virus-related hepatocellular carcinoma. J Viral Hepat. 2010;17:287–92. doi:10.1111/j.1365-2893.2009.01181.x.
32. Arase Y, Ikeda K, Suzuki F, Suzuki Y, Kobayashi M, Akuta N, et al. Interferon-induced prolonged biochemical response reduces hepatocarcinogenesis in hepatitis C virus infection. J Med Virol. 2007;79:1485–90. doi:10.1002/jmv.20925.
33. Nomura H, Kashiwagi Y, Hirano R, Tanimoto H, Tsutsumi N, Higashi M, et al. Efficacy of low dose long-term interferon monotherapy in aged patients with chronic hepatitis C genotype 1 and its relation to alpha-fetoprotein: a pilot study. Hepatol Res. 2007;37:490–7. doi:10.1111/j.1872-034X.2007.00073.x.
34. Chen TM, Huang PT, Tsai MH, Lin LF, Liu CC, Ho KS, et al. Predictors of alpha-fetoprotein elevation in patients with chronic hepatitis C, but not hepatocellular carcinoma, and its normalization after pegylated interferon alfa 2a-ribavirin combination therapy. J Gastroenterol Hepatol. 2007;22:669–75. doi: 10.1111/j.1440-1746.2007.04898.x.
35. Osaki Y, Ueda Y, Marusawa H, Nakajima J, Kimura T, Kita R, et al. Decrease in alpha-fetoprotein levels predicts reduced incidence of hepatocellular carcinoma in patients with hepatitis C virus infection receiving interferon therapy: a single center study. J Gastroenterol. 2012;47:444–51.

EXPERIMENTAL CELL RESEARCH 319 (2013) 35–44

Available online at www.sciencedirect.com

SciVerse ScienceDirect

journal homepage: www.elsevier.com/locate/yexcr

Research Article

Involvement of hepatocellular carcinoma biomarker, cyclase-associated protein 2 in zebrafish body development and cancer progression

Kathryn Effendi[a], *Ken Yamazaki*[a], *Taisuke Mori*[a], *Yohei Masugi*[a], *Shinji Makino*[b], *Michiie Sakamoto*[a,*]

[a]*Department of Pathology, School of Medicine, Keio University, 35 Shinanomachi, Shinjuku-ku, Tokyo 160-8582, Japan*
[b]*Department of Regenerative Medicine and Advanced Cardiac Therapeutics, Center for Integrated Medical Research, School of Medicine, Keio University, Tokyo, Japan*

ARTICLE INFORMATION

Article Chronology:
Received 20 April 2012
Received in revised form
20 August 2012
Accepted 10 September 2012
Available online 27 September 2012

Keywords:
Skeletal muscle
Actin
Cancer
Development
HCC cells
Zebrafish

ABSTRACT

Cyclase-associated protein 2 (CAP2) is a conserved protein that is found up-regulated in hepatocellular carcinoma (HCC). By using zebrafish, combined with HCC cell lines, we further investigated the role of CAP2. The zebrafish CAP2 sequence was 60% identical to human CAP2 with 77% homology in the C-terminal actin-binding domain, and 58% in the N-terminal cyclase-binding domain. CAP2 expression was observed during zebrafish development and was preferentially expressed in the skeletal muscle and heart. Knockdown using two different morpholinos against CAP2 resulted in a short-body morphant zebrafish phenotype with pericardial edema. CAP2 was observed co-localized with actin in zebrafish skeletal muscle, and in the leading edge of lamellipodium in HCC cell lines. CAP2 silencing resulted in a defect in lamellipodium formation and decreased cell motility in HCC cell lines. Strongly positive expression of CAP2 was observed in 10 of 16 (63%) poorly, 30 of 68 (44%) moderately, and 2 of 21 (10%) well differentiated HCC. CAP2 expression was significantly associated with tumor size, poor differentiation, portal vein invasion, and intrahepatic metastasis. Our results indicate that an important conserved function of CAP2 in higher vertebrates may be associated with the process of skeletal muscle development. CAP2 also played an important role in enhancing cell motility, which may promote a more invasive behavior in the progression of HCC. These findings highlight the link between development and cancer.

Introduction

Hepatocellular carcinoma (HCC) is the sixth most common malignancy in the world and ranks as the third highest cause of cancer-related death globally [1]. HCC is characterized by an obvious multistage process of tumor development, and as with other cancers, diagnosis of early stage HCC is important for appropriate treatment. Previously, we reported that the cyclase-associated protein 2 (CAP2) gene was upregulated in early HCC [2]. CAP was originally identified in the budding yeast, *Saccharomyces cerevisiae*,

*Corresponding author. Fax: +81 3 3353 3290.
E-mail address: msakamot@z5.keio.jp (M. Sakamoto).

0014-4827/$ - see front matter © 2012 Elsevier Inc. All rights reserved.
http://dx.doi.org/10.1016/j.yexcr.2012.09.013

as a factor required for RAS-activated adenylate cyclase activity [3,4], and since then, at least two homologs of CAP, CAP1 and CAP2 have been found in mammals [5–8]. In yeast, the amino (N)-terminal domain of CAP interacts with adenylyl cyclase and is necessary for the cellular response to activate RAS protein. The carboxyl (C)-terminal domain, on the other hand, appears to play a role in nutritional responses and actin distribution, and is necessary for normal cellular morphology [9–11]. Comparing human or rat CAP protein with yeast indicates that only the C-terminal functions of CAP are highly conserved [5,7]. However, the mechanisms underlying actin regulation by CAP are not yet completely understood. The conservation of CAP functional properties in mammals or higher vertebrates suggests that there are still some unrevealed functions of CAP. The CAP homolog, CAP1 is well studied [12,13] compared with CAP2. Interestingly, we found upregulation of CAP2 in early stage HCC [2], and its expression was related to the multistage development of hepatocarcinogenesis [14]. *CAP2* overexpression has not been previously reported in human cancer. Thus, our previous studies indicated an intriguing function of *CAP2* in HCC, as well as in mammals, which requires further exploration.

Recently, the zebrafish (*Danio rerio*) widely used in developmental studies has emerged as a novel vertebrate model to study cancer susceptibility and carcinogenesis, since they offer combined advantages of invertebrate and mammalian models. They have large clutch sizes, and rapid embryonic development. Organogenesis is easy to examine *in vivo* and in real time. High similarities between the histology of normal and malignant zebrafish tissue to that of mouse and human samples has made zebrafish an excellent model system for cancer [15,16]. Also, the ability to perform large-scale 'reverse' genetics using morpholino synthetic anti-sense oligonucleotides which effectively 'knockdown' gene activity in the zebrafish embryo has further popularized their use as a model system [17,18]. The contribution of zebrafish to the cancer field is still growing. Many approaches to induce tumor formation in zebrafish have been established, and non-invasive methods to image tumor development using the transparent adult zebrafish have also recently been developed [19,20]. Thus, zebrafish have now emerged as a new favorite model to study both development and cancer.

In this study, we examined the expression of CAP2 during zebrafish development and utilized morpholino antisense oligonucleotides for protein knockdown studies in zebrafish. We also investigated the functional role of CAP2 using HCC cell lines and further examined CAP2 expression in HCC clinical specimens.

Material and methods

Embryo collection

Zebrafish embryos were obtained by natural mating of RIKEN wild-type zebrafish (*Danio rerio*). Collected embryos were maintained in egg water (5 mM NaCl, 0.17 mM KCl, 0.33 mM $CaCl_2$, 0.33 mM $MgSO_4$, 10^{-5}% methylene blue) at 28.5 °C and embryos were staged using standard morphological criteria [21]. Embryos were gently dechorionated using watchmaker's forceps.

Tissue resection

Adult zebrafish were anesthetized with tricaine (1:20 dilution in clean tank water) and placed on a sponge. Resection was performed under brightfield imaging on a dissection microscope. The incision was made through the ventral body wall and posterior to the heart using microdissection scissors. The brain, eye, heart, abdominal organs, and skeletal muscle were resected using forceps and quickly placed in lysis buffer for Western blot analysis, or frozen in liquid nitrogen for RNA extraction.

Morpholinos and microinjections

Morpholino antisense oligonucleotides were obtained from Gene Tools LLC (Oregon, USA). Two non-overlapping CAP2 antisense morpholinos, and each corresponding five-mispair control morpholinos were designed: (A) ATG-MO (5′-GACGACCAACCAGAGCCTCCATAAC-3′), with its control (5′-GAgGAgCAACCACCAcAGCCTCgATtAC-3′) and (B) UTR-MO (5′-ATATTACCTCAGATGGTGTGGCCCG-3′), with its control (5′-ATtTTACCTgAGATcGTGTaGCgCG-3′). The sequence of CAP1 antisense morpholino was as follows: ATG-MO (5′-ATCTGCCATGCCGTCGCCGTGTGAA-3′), with its five-mispair control (5′-ATgTGCgATGCCcTCGCCcTGTcAA-3′). The sequence used for standard control was 5′-CCTCTTACCTCAGTTACAATTTATA-3′. Morpholino oligonucleotides were stored in 1.0 mM concentration and were diluted to working concentrations in 1 × Danieau's buffer. A dose range of 0.1–1 mM ATG-MO was defined as effective and specific window of concentration which resulted in comparable specific phenotypes. We used 0.3 mM as our choice of morpholino concentration. For the double knockdown approach, CAP2 and CAP1 morpholinos were mixed in a 1:1 ratio (0.3 mM). Fertilized embryos were injected at the 1–8 cell stages into the cytoplasmic streaming of the yolk with 1–2 nL of solution containing either morpholino, or its mispair control. They were allowed to develop in egg water maintained at 28.5 °C. Developed embryos were photographed using a Leica M275 microscope and further evaluated by Western blot and immunohistochemical analysis.

Western blotting

Lysates of HCC cancer cells, adult male zebrafish organs, and zebrafish larva were gently homogenized in lysis buffer (50 mM Tris–HCl (pH 7.4), 250 mM NaCl, 5 mM EDTA, 1% NP-40 (IGEPAL), 10% glycerol, 1 mM DTT, and 25 × protease inhibitor). After determining protein concentrations using the Quant-iT™ Protein Assay Kits (Invitrogen, Eugene, OR), lysates were loaded onto and separated on SDS-PAGE (4–12% Bis-Tris gel; Invitrogen, Carlsbad, CA), and transferred to PVDF membrane using the semi-dry blotting method. The membranes were blocked with 5% nonfat dry milk and probed with our originally raised rabbit polyclonal antibodies against human CAP2 (1/500), CAP1 (1/200) [14], and a mouse monoclonal beta actin antibody (1/1000; Sigma-Aldrich, St. Louis, MO, USA) as a loading control. Horseradish peroxidase-conjugated secondary antibodies were used to probe the membranes and visualized with ECL western blotting detection reagents (GE Healthcare, UK Ltd., Buckinghamshire, UK).

Immunohistochemical analysis

Zebrafish specimens were fixed in 4% paraformaldehyde-PBS at 4 °C overnight and embedded in paraffin tissue section. For staining, slides were deparaffinized and rehydrated, and sections were heated at 120 °C in 0.1 mM Tris–HCl buffer (pH 9.0) for 10 min using an autoclave. The sections were incubated with

rabbit anti-human CAP2 (1/4000), and CAP1 (1/2000), followed by ImmPRESS anti-rabbit Ig Kit secondary antibody (Vector Laboratories, Burlingame, CA). A rabbit immunoglobulin (1/50000; DAKO X0936, Glostrup, Denmark) was used as a negative control. The sections were counterstained with hematoxylin and then mounted. Immunohistochemical staining for HCC clinical specimens was done on formalin-fixed, paraffin-embedded tissue sections according to the methods previously described [14]. Staining analysis was done at least twice. Smooth muscle of the vascular wall served as the internal positive control. We defined CAP2 staining criteria as follows: intensity stronger than or equal to the positive control with more than 50% positive cell in each lesion was scored 2+, while less than 50% positive cell was scored 1+; intensity weaker than the positive control with positive cell more than 50% was also scored 1+, and with positivity less than 50% was considered negative. According to the previous result of CAP2 expression in HCC [14], we used 50% as a cut-off value to divide the HCC cases into high and low positivity group.

Tissue specimens of HCC

HCCs and corresponding non-cancerous liver tissue were obtained from 91 patients with 105 nodules (21 well differentiated (including 9 early), 68 moderately differentiated, and 16 poorly differentiated HCCs) who underwent surgical resection at Keio University Hospital (Tokyo, Japan) between 2003 and 2006. The histological diagnosis was made according to the criteria set by the World Health Organization [22]. This study was approved by the Ethics Committee of Keio University School of Medicine.

Cell culture

The human HCC cell line, PLC/PRF/5, was obtained from the American Type Culture Collection (Manassas, VA). KYN-2 was established as reported previously [23]. All the cells were grown in RPMI 1640 medium supplemented with 10% fetal bovine serum, 100 U/mL penicillin, and 100 μg/mL streptomycin.

Immunocytochemical analysis

PLC/PRF/5 and KYN-2 cells were grown to confluence on glass slides, fixed with 3.7% formaldehyde, and permeabilized with 0.1% Triton X-100 in phosphate buffered saline. The slides were incubated overnight at 4 °C with CAP2 antibody (1/100). After rinsing, the slides were covered with FITC-labeled secondary antibody (Dako, Glostrup, Denmark) with rhodamine-phalloidin and Hoechst 33342 dye (Invitrogen), and visualized using an Axiovert 200 microscope, and AxioCam CCD camera (Carl Zeiss MicroImaging Inc., Tokyo, Japan). For negative control, PLC/PRF/5 was incubated without primary antibody, and visualized using the LSM 510 Meta confocal microscope (Carl Zeiss, Oberkochen, Germany). All staining analysis was done at least twice.

RNA interference and serum stimulation analysis

Two small interfering RNA (siRNA) targeting two CAP2 sequence (siCAP2A and siCAP2B) were synthesized by B-Bridge International, Inc. The target sequences were GGAGUGAACUUCAAGCAUA and GGAGUUGGAAGGAAAGAAA. Cells were cultured until 70–80% confluence onto collagen I-coated six-well plates, and were transfected with siRNA using the DharmaFECT General Transfection Protocol (Dharmacon, Thermo Fisher Scientific, Lafayette, CO, USA). A non-targeting siRNA pool (QIAGEN, Valencia, CA, USA) was used as a negative control. Cells were incubated at 37 °C, 5% CO_2 for 48 h, and to observe lamellipodium formation, the transfectants were serum starved for 24 h. On the following day, the serum was changed with medium supplemented with 10% FBS for 30 min.

Semi-quantitative RT-PCR analysis

Purification of RNA from each zebrafish tissue samples was accomplished by isolation through Isogen (Nippon Gene Co. LTD, Toyama, Japan), and cDNA was synthesized using the PrimeScript RT reagent Kit (Takara Bio, Shiga, Japan). As a template for amplification, 10 μL of each sample was used. A primer set designed for zebrafish CAP2 expression amplified a 175 base pair fragment (5′-GGCTGATTGATCTGCCTCCTC-3′ and 5′-AAGCACAGTGGGTCTGGGG-3′), and a primer set targeting zebrafish CAP1 amplified a 179 base pair fragment (5′-GATGGCTGCCACGTGTACCT-3′ and 5′-ATCTCGGTGGCTGTGGTGAC-3′). Each reaction was run on 2% agarose in 1 × TAE buffer.

Migration assay

PLC/PRF/5 and KYN-2 cells transfected for 48 h with siCAP2A, siCAP2B, and negative control siRNA were suspended in medium supplemented with 0.5% FBS. Cells treated with each siRNA were dispersed in each of three independent upper chambers of BD BioCoat Control Culture Inserts (pore size = 8 μm; BD Biosciences, San Diego, CA, USA). Chemoattractant medium containing 10% FBS was added to the bottom plate. After 24 h incubation, non-migrated cells were removed by scrubbing with cotton-tipped swabs and migrated cells were stained with Diff-Quick stain (Kokusai Shiyaku, Kobe, Japan). The number of migrated cells on three independent membranes was counted under microscope. The ratio of the number of migrated cells represents the mean number of migrated cells with each siRNA treatment, divided by the mean number of migrated control cells.

Statistical analysis

The chi-squared test was used when appropriate to determine the correlations between clinicopathological variables and CAP2 expression. Statistical significance was defined as $P<0.005$. All statistical analyses were carried out using SPSS statistical software (SPSS, Chicago, IL, USA).

Results

CAP2 is expressed in both the embryo and adult zebrafish

The conservation of CAP2 from yeast to mammals suggests that CAP2 also exists in zebrafish. We examined CAP2 presence in zebrafish and found that the zebrafish Cap2 sequence (LOC393809; NP_957130.1) was 60% identical to the already known human CAP2, with 77% homology in the C-terminal actin-binding domain, 57% in the middle proline-rich sequence, and 59% in the N-terminal